RSC Advances

ROYAL SOCIETY OF CHEMISTRY

www.rsc.org/advances

Journal Name

ARTICLE

The Effect of Prefrozen Process on Properties of Chitosan/ Hydroxyapatite/ Poly(methyl methacrylate) Composite Prepared by Freeze Drying method Used for Bone Tissue Engineering

Received 00th January 20xx,
Accepted 00th January 20xx

DOI: 10.1039/x0xx00000x

www.rsc.org/

Xueqing Zhang, Yuxuan Zhang, Guiping Ma, Dongzhi Yang and Jun Nie*

A chitosan-hydroxyapatite (CS-HA) scaffold reinforced by poly(methyl methacrylate) (PMMA) with good mechanical strength were fabricated. Chitosan-hydroxyapatite scaffolds supplemented with poly(methyl methacrylate) were fabricated by freeze drying technology and free redical polymerization. Possible applications of the prepared CS-HA/PMMA scaffolds in tissue engineering were tested. The effect of freeze drying process and chitosan concentration on properties of the scaffolds had been investigated. The morphology of CS-HA scaffolds was examined by scanning electron microscopy (SEM). The thermal property of the complex scaffolds was examined by thermogravimetry analysis (TGA). The mechanical property of bone composites was characterized by an Instron 4505 mechanical tester. Indirect in vitro cytotoxicity test showed that the extracts of bone composites had no significant effects on cell viability. Moreover, in vitro cytocompatibility test also exhibited cell population and spreading tendency, suggesting that CS-HA/PMMA scaffolds were non-toxic to L929 cells. All the results indicated that not only the freeze drying method had significant influence on the property of complex scaffolds, but also the chitosan concentration had significant influence on the property of complex scaffolds. The proposed method could be used to fabricate CS-HA/PMMA bone composites by freeze drying and free redical polymerization, and the fabricated bone composites might have potential applications in bone tissue engineering scaffolds field.

1. Introduction

There are people suffering from bone defects from tumour, trauma or bone related diseases every year, some of them would even die because of insufficient of ideal bone tissue.[1] During the past decades, autologous and allogenous bone grafts had been used mostly as their advantages such as little immune response and good healing.[2] However, autologous grafts and allogenous grafts possessed the risk of disease transmission and donor site morbidit.[3] The limitations in using autologous or allogenous bone grafts has led to the consideration of bone tissue engineering.[4]

The main purpose of bone tissue engineering is to create implantable 3D bone substitutes used for skeletal defects and present the current status of translational approaches to engineering bone regeneration.[5]

Chitosan (CS), a natural cationic polysaccharide, is widely used in combination with polylactic acid or collagen to develop scaffolds for tissue engineering due to its nontoxicity, biofunctionality, biocompatibility and antibacterial nature.[6-8] Chitosan-based biomaterials have undergone numerous innovations in the field of tissue engineering and biomedical applications. The valuable aspects of chitosan products including biocompatibility and biodegradability have made chitosan an inevitable source for tissue engineering biomaterials.[9] Tissue engineering biomaterials should be biocompatible with appropriate surface chemistry for cell attachment and proliferation. Many studies have been focused on the fundamental performance of chitosan, such as molecular weight of components on particles sizes, mechanical properties and network structure of biological tissues, so chitosan had been widely used in the biomedical field.[10] For example, it was preferable that a tissue engineering construct served as both a delivery carrier and a three-dimensional (3-D) porous scaffold for cellular activities.[11]

Hydroxyapatite (HA) is the calcium phosphate mineral found in vertebrate bones, mammalian teeth, fish scales, and the mature teeth of some chitosan species.[12] HA is well known for its excellent bioactivity and biocompatibility and has been used in bone tissue engineering currently.[13] Furthermore, the osteoconduction, non-inflammation and non-toxicity of HA enable osteoblast adhesion, proliferation and differentiation.[14] HA has a unique ability of binding to the natural bone through biochemical bonding, which promotes the interaction between host bone and grafted material.[15,16] It was also demonstrated that bone had a greater affinity for implants containing high

State Key Laboratory of Chemical Resource Engineering, Beijing Laboratory of Biomedical Materials, Beijing University of Chemical Technology, Beijing 100029, PR China. E-mail: junnie@mail.buct.edu.cn; Fax: +86-01064421310; Tel: +86-01064421310

percentages of HA than those with trace amounts or none through the in vivo experiment[17]. However, it is difficult to handle HA and keep HA in defect sites because of the brittleness and low plasticity of HA.[18]

Ice segregation induced self-assembly (ISISA) as a freeze casting technique is a green bottom-up method to produce aligned macroporous or layered materials in a sophisticated architecture.[19-21] Freezing causes solute or solids in a solution, emulsion, or dispersion to be excluded by an advancing ice front into the interstitial spaces between ice crystals. Subsequent sublimation leads to porous structures.[22] By controlling concentration and freezing direction, complex hierarchical morphologies are produced, including well-aligned channels, honeycombs, and brick-mortar-bridges. Guiping Ma et al. reported chitosan-sodium hyaluronate polyelectrolyte complex fibres for tissue engineering scaffolds fabricated by freeze drying technique.[23] Applications of freeze drying structures are numerous. Not only can these structures be used in diverse technologies such as microfluidics and continuous flow catalysts, but can also be used in tissue regeneration.[22] Most studies focused on the freezing in a low temperature environment, but no comparison between directional freezing under liquid nitrogen and freezing under a slowly cooling method.

In order to overcome the brittleness of hydroxyapatite, chitosan-hydroxyapatite scaffolds can be fabricated by phase separation and lyophilization technique, rapid prototyping technology, electrospinning.[23] Researchers have done plenty works to overcome the drawbacks such as low mechanical strength，brittleness and low biocompatibility. Chellan Rose et al. reported a collagen chitosan composite scaffold for tissue engineering with a better mechanical property.[24] Jing Han et al. fabricated a porous PMMA scaffold which had good mechanical property matched with natural bone well.[25] Zhang, Venugopal, El-Turki, Ramakrishna, Su and Lim prepared biomimetic nanofiber of CS-HA by combining an in situ co-precipitation synthesis approach with an electrospinning process. It was demonstrated that cells could adhere and proliferate well.[26] Almeida, Leite, Loureiro, Correia, and Santos[27] prepared a new poly (methyl methacrylate)-co-ethylhexylacrylate (PMMA-co-EHA) bone cement which showed excellent biocompatibility.[27] Jiang. et al.[17] had prepared n-HA/CS scaffold by freeze-drying with better cell biocompatibility than chitosan scaffold in vitro. Ran Kang et al. prepared human induced pluripotent stem cells seeded biomimetic nano-hydroxyapatite (nHAp) contained polycaprolactone (PCL) nanofibers scaffolds which was excellent for bone regeneration.[28] M. S. Fernández prepared a novel porous multilayered 3D chitosan–hydroxyapatite composite scaffold enriched with fibronectin or extracellular matrix which could improve proliferation and differentiation of osteoblas.[29]

But the mechanical strength was still not enough for application. The main purpose of this work was to develop a chitosan-hydroxyapatite scaffold which is reinforced by poly(methyl acrylate) and compare the influence of different freeze drying process and different chitosan concentration on the properties of bone composites. And also to develop a potential bone substitute which has both good biocompatibility and good mechanical properties. As a bone-inducing biopolymer, chitosan was utilized as a framework. HA acted as a high biocompatibility component which can form a direct bond with bone. PMMA acted as the load-bearing part. The mechanical properties, thermal stability of the prepared composites were characterized. The adhesion and proliferation of L929 cell were also measured. It demonstrated that our scaffolds not only had a good mechanical property, but also had a good biocompatibility.

2. Experimental Section

2.1 Materials

Chitosan (CS, molecular weight of 50000 g/ mol, about 85% deacetylated) was purchased from Zhejiang Golden-Shell Biochemical Co., Ltd. (Zhejiang, China). Hydroxyapatite (HA, particle size of 60nm, about 96% pureness) was purchased from Shanghai Pucheng Biochemical Co., Ltd. (Shanghai, China). Methyl methacrylate (MMA, Tianjin Fuchen Chemical Co., Ltd) was purified by distillation under reduced pressure. Benzoyl peroxide (BPO) and N, N-bis (2-hydroxyethyl)-ptoluidine (BHET) were obtained from Xilong Chemical Co., Ltd. (Shantou, China) and Fluka Chemical Co., Ltd respectively. N-hexane was purchased from Sinopharm Group Chemical Reagent Co. (Beijing, China). 3-(4,5-dimethylthiazol-2-yl)-2,5-diphenyltetrazolium bromide tetrazole (MTT) was obtained from Alfa Aesar (Massachusetts, USA). Dulbecco's modified eagle medium (DMEM) and Fetal calf serum (FBS) were purchased from Shanghai Luwen Biochemical Co., Ltd. (Shanghai, China). Phosphate Buffered Saline (PBS) was purchased from Qingdao Haibo Biochemical Co., Ltd. (Qingdao, China). Dimethyl sulfoxide and phenol were purchased from Sinopharm Chemical Reagent Co., Ltd. (Shanghai, China). Benzoyl peroxide(BPO) was purified by fractional precipitation from a chloroform solution, using methanol as precipitant.

2.2 Method

2.2.1 Preparation of CS-HA scaffolds

CS-HA scaffold was prepared by freeze drying. The compositions of the mixture are summarized in Table 1. First, chitosan was dispersed in acetic acid aqueous solution (2% acetic acid dissolved in deionized water) and stirred for 30min. Then HA nanoparticles were added to the resultant chitosan solution and dissolved by vortexing for 30 min and sonicating for 10 min more. The obtained solution was injected into a cylindrical mould with 10mm diameter and 50mm height and was divided into two groups and denoted as group 1 and group 2. Group1 was put into liquid nitrogen until the solution was totally frozen. This procedure was denoted as rapidly cooling method (RCM). Group 2 was placed in a refrigerator whose temperature was -40 ℃ for 24 h. This procedure was

denoted as slowly cooling method (SCM). After that, all the samples were freeze-dried in a 680 (width) *830 (length) *380 (height) mm^3 tube, which was connected to a Lyovac GT-10 freeze-dryer (Beijing Songyuan-Huaxin Technology Develop CO., Ltd) for 48 h.

Preparation of CS-HA/PMMA composites

CS-HA/PMMA bone composite was synthesized by free redical polymerization. MdMA solution with photoinitiator BPO and coinitiator BHET was prepared as follows: photoinitiator BPO (1% w/w) and co-initiator BHET (1% w/w) were dissolved in MMA, and stirred for 5min to achieve a homogenous solution. Then the resultant solution was injected into the porous CS-HA scaffold rapidly and ultrasonicated for 5 min so that MMA solution could be dispersed uniformly in the CS-HA scaffold. Free redical polymerization of MMA took place in the porous scaffold at room temperature. Cylindrical CS-HA/PMMA bone substitute composite was obtained after 12 h.

2.3 Characterization

2.3.1 Porosity studies

The porosity of different CS-HA scaffolds were measured by Archimedes liquid displacement method using n-hexane at room temperature. CS-HA scaffold was cut into discs with a diameter of 10 mm and a thickness of 20 mm. First, 5 mL n-hexane was placed into cylindrical mould. Then the disc was immersed into n-hexane for 6 h to make sure the disc was saturated. Then, the disc was taken out. The volume of n-hexane before and after the immersing of CS-HA disc was measured. The porosity was calculated by using the following formula,

$$\mathbf{p} = \frac{V_1 - V_3}{V_2 - V_3}$$

where V_1 was the volume of the original n-hexane, V_2 was the volume of n-hexane after the disc was immersed in and was measured immediately, and V_3 was the volume of n-hexane which was measured after the disc was taken out.

2.3.2 Morphologies of porous scaffolds

The microstructure of CS-HA scaffolds was observed by scanning electron microscopy using a Hitachi S-4700 microscope, wherefore the sample was fixed by sputtering on gold-coated stubs before the measurement.

2.3.3 Thermogravimetric analysis

Thermogravimetric analysis was performed on a TA Q500 (TA Instruments). Each sample was grind into powder and put in a platinum copple. The experiment was run from room temperature to 800 ℃ at a heating rate of 10 ℃/min under 50 mL/min nitrogen flow.

2.3.4 XRD

The crystallinities of CS-HA/PMMA scaffolds were identified by using a Rigaku D/Max2500VB_2^+/Pc diffractometer (Rigaku Company, Tokyo, Japan) at 40 kV and 50 mA with Cu Ka radiation (λ = 0.154 nm). The scanning scope of 2θ was 10°–70° and the scanning rate was 5°/min.

2.3.5 Mechanical compression testing

The compression modulus of CS-HA/PMMA composites was determined by using an Instron 4505 mechanical tester (Instron, High Wycombe, England) with a 10 kN load cell. The specimens were circular discs of 8 mm in diameter and 12 mm in thickness. The crosshead speed of the Instron tester was set at 5 mm/min and the load was applied until a 30% reduction in specimen height was achieved. Five samples were tested for each sample.

2.3.6 Cytotoxicity assay

To evaluate cytotoxicity of CS-HA/PMMA scaffolds, MTT assay was used.[30] In this technique, the yellow tetrazolium salt MTT is reduced to a purple formazan compound by the dehydrogenase activity of intact mitochondria. Consequently, this conversion only occurs in living cells. For the purpose of this assay, all samples used in cytotoxicity assay were previously sterilized by high temperature in a hermetically sealed instrument. After sterilization, CS-HA/PMMA scaffolds samples were placed into 200 mL DMEM (Dulbecco's modified Eagle's medium) with 10% FBS (fetal bovine serum) for 48 h at 37℃ and different concentrations of their extract liquid were obtained from the medium. Then, the mouse fibroblast L929 cells were seeded in 96-well tissue culture plates at an initial density of 1×10^4 cells per well. A final volume of 100 µL of cultured medium per well containing DMEM were used. Cultures were incubated for 24 h in a humidified atmosphere of 95% air and 5% CO_2, at 37 °C. The CS-HA/PMMA scaffolds (Φ=5mm, h=2mm) prepared by different prefrozen methods and different chitosan concentration were then added in the confluent layer of L929 cells. After 24, 48 and 72 h of incubation period, 20mL of MTT solution (5 mg/mL in PBS) was added to each well followed by incubation in a humidified atmosphere at 37 °C for 4 h. For dissolution of the purple formazan crystals formed after the incubation period, 150 mL of the solubilization solution (DMSO) was added and incubated overnight in a humidified atmosphere at 37 °C. The optical density (OD) of each well at the absorbance wavelength of 595 nm was determined by a microplate reader at a test wavelength of 490 nm. The cell viability was estimated in the form of percentage of the absorbance with respect to the control experiment without using CS-HA/PMMA scaffolds. Phenol was used as the positive control and culture medium containing 0.1% DMSO was used as the negative control.

2.3.7 Cell Attachment and Proliferation Studies

The attachment and spreading nature of L929 mouse fibroblasts on the CS-HA/PMMA composites were evaluated using SEM. The CS-HA/PMMA composites were first fixed on the glass slide. The sample was sterilized, rinsed three times by using sterile phosphate buffer solution (PBS), and then transferred to individual 24-well tissue culture plates. Aliquots (1 mL) of Fibroblasts cells suspension with 1.5×10^4 cells/mL were seeded on the samples. After 24 h of incubation, cellular constructs were harvested and rinsed twice with PBS to remove non-adherent cells. Then they were fixed with 2.5% glutaraldehyde solution for 4h at 4℃. After being thoroughly washed with PBS, the samples were dehydrated in a serious of graded ethanol and dried over night at room temperature. The dried samples were coated with gold for further cell morphology analysis by SEM.

3. Results and discussion

3.1 Morphology and Porosity

Investigation of the morphology of the CS-HA scaffolds by SEM (Figure 1) showed that both the prefrozen method and ratio of chitosan had significant influence on the porosity and microstructure of the scaffolds. The scaffolds which were fabricated by SCM had uniform and well interconnected pores. But the scaffolds which were fabricated by RCM had disordered and disconnected pores. The sample codes and porosity of each sample are shown in Table 1.

SEM results corresponded to the porosity results well. In the table, the porosity of CS-HA scaffolds which were prefrozen in liquid nitrogen was 33.8%, 45.8%, 47.0%, 51.7% corresponded to CS-12/HA-10, CS-9/HA-10, CS-6/HA-10 and CS-3/HA-10 respectively. The porosity of CS-HA scaffolds which were prefrozen at -40 ℃ was 47.0%, 50.3%, 55.3%, 62.1% corresponded to CS-12/HA-10, CS-9/HA-10, CS-6/HA-10 and CS-3/HA-10 respectively. The porosity of CS-HA scaffolds decreased within the increase of chitosan content. Both the porosity of CS-HA scaffolds prepared by SCM and RCM decreased with the increase of chitosan content. The initial volume of the frozen chitosan solutions with different chitosan concentration were the same. As the chitosan concentration increased, the corresponding volume of chitosan increased so that the volume of ice decreased. In Figure 1, a, b, c and d corresponded to CS-3/HA-10, CS-6/HA-10, CS-9/HA-10 and CS-12/HA-10 prepared by SCM, respectively. Image e, f, g and h corresponded to CS-3/HA-10, CS-6/HA-10, CS-9/HA-10 and CS-12/HA-10 prepared by RCM, respectively. The variation trend of porosity accorded with the variation trend morphology well. The CS-HA scaffolds prepared by SCM consisted of a three-dimensional interconnected and ordered pore structure, based on SEM images (Figure1a–1d). But the CS-HA prepared by RCM had a random porous architecture (Figure1e-1h). These results may due to the dissolution process of chitosan and the ice crystallization process.

The proposed mechanism for formation of chitosan network structures and the microstructure of scaffolds are illustrated in Scheme 1 and Figure 2. Natural chitosan has a complex inter- and intra-molecular hydrogen-bond network, which makes it insoluble in water and leads to the chitosan molecule being curled.[31] When chitosan was dissolved in the acetic acid, the amino groups on chitosan was protonated. Chitosan was well dispersed in acetic solution due to strong electrostatic repulsion.[32] Ice crystallization is consisted of crystal nucleation and crystal growth. Ice nucleation rate is determined by the degree of supercooling, whereas the ice growth rate is largely controlled by the rate of heat transfer from the crystal surface to the bulk water.[33] When the chitosan solution was put into a refrigerator, ice starts to nucleate and grow. Initially, chitosan chains were pushed together by the advancing ice fronts, leading to interactions such as van der Waals attraction, electrostatic repulsion, and hydrogen bonding. Dissolved chitosan chains tend to be excluded from the ice phase during freezing, since the solubility of a solute in ice is almost negligible.[34] At this stage we propose that individual chitosan assemble into interconnected pores. As ice continues to grow slowly, these chitosan started to form a three-dimensional aperiodic network structure which then becomes columnar or lamellar structures later as shown in Figure 1a-1d. Next, the ice crystals were directly sublimated into water vapour, the solute molecules were left and became the CS-HA scaffolds.

For the RCM, columnar ice phases are preferred to disordered lamellar ice crystals as shown in Figure 1. From Figure 1e to Figure 1h, lamellar structure turned into totally disordered porous structure. Rapid freezing can cause dendrite formation. However, if the velocity of ice growth is fast enough, dendritic structures can break down, allowing solutes to become entrapped in the solid rather than excluded to the inter-dendritic region.[35] This is the reason why the scaffold prepared by RCM had disordered and dis connected pores. The porosity of scaffolds prepared by SCM were higher than prepared by RCM is due to the connectivity of the pores in the scaffolds. The scaffold prepared by SCM is of a three-dimensional aperiodic network structure which is internal connected. The scaffold prepared by RCM is of a disordered network which is not internal connected. Therefore, the porosity of scaffolds prepared by SCM were higher than that prepared by RCM.

3.2 Thermogravimetric analysis

The thermal behaviour of the prepared scaffolds was investigated by thermogravimetric analysis (TGA). The TGA and DTG curves of CS-HA/PMMA scaffolds and bulk PMMA were shown in Figure 3. The residual weight ratio of bulk PMMA was 0.3% which belongs to the residual weight of carbon. The residual weight ratio of CS-HA/PMMA scaffolds which were prepared by SCM was 11.60% after thermal degradation. The residual weight ratio of CS-HA/PMMA scaffolds which were prepared by RCM was 13.13% after thermal degradation. The residual weight correspond to the weight of HA and residual carbon. The thermogravimetric behaviour of CS-HA/PMMA scaffolds fabricated by different methods were almost the same. As shown in Figrue3a, bulk PMMA had an onset degradation temperature at 326 ℃ and lost nearly all weight at 428 ℃. The degradation of PMMA consisted of three stages. The first stage (150 – 200 ℃) corresponded to a degradation initiation due to the breaking of weak head to head linkage due to its instability. The second (250 – 300 ℃) stage was due to the degradation initiated by the unsaturated ends of radical polymerized PMMA. The last stage (350 ℃) was caused by the random chain scission of PMMA.

The degradation behaviour of CS-HA/PMMA composite was different from that of bulk PMMA. The scaffolds had two degradation stages at 300 ℃ and 395 ℃ (Figure 3b), respectively. The former temperature was ascribed to the part degradation of chitosan; the latter temperature corresponded to the degradation of PMMA. Compared with bulk PMMA, the presence of CS and HA offered a stabilizing effect for PMMA since the onset of degradation occurred at a high temperature. The residual mass at 400 ℃ for bulk PMMA was nearly 0%, while that for bone composite was still 35.68%. The data implied that the presence of CS and HA hindered the unzipping of the PMMA. The retardation effects might attribute to the

interaction between CS and macro-radicals generated during the degradation process.

The residual mass ratio at 600°C for CS-HA/PMMA was nearly 10%, almost equal to the content of HA before freeze drying. The curves also showed that the prefrozen methods had no significant influence on the thermal behaviour of the prepared composites.

3.3 Mechanical compression testing

The mechanical property of materials plays a vital role in determining the long-term stability of biomaterials. The compression modulus of different CS-HA/PMMA scaffolds was shown in Figure 4. It indicated that the compression modulus was significantly influenced by the CS content and prefrozen method. The compression modulus of the scaffolds improved with the increase of chitosan. This was attributed to the uniform dispersion of chitosan in PMMA and the reinforcement of effect of chitosan. Chitosan, as a rigid and semicrystallized oligomer played an important role in improving mechanical strength of two-continuous phase composites. CS-HA/PMMA scaffolds prepared by SCM had much higher compression modulus than that of the scaffolds prepared by RCM. During the MMA injecting procedure, the scaffolds prepared by SCM had interconnected pores so that MMA could combine well with CS-HA scaffolds. This insured that the PMMA had continuous phase to provide a higher compression modulus. But the scaffolds prepared by RCM had disconnected pores and the polymerized PMMA did not behave as continuous phase which was bad for the material's compression modulus.

3.4 XRD

Figure. 5 shows the wide-angle X-ray diffractograms of CS-HA/PMMA scaffolds. Bone scaffolds prepared by SCM and RCM both showed typical HA peaks. Peak at $2\theta = 13^{o}$ in the XRD could be ascribed to chitosan. Peaks in the XRD spectra could be ascribed to HA, with the major peaks at $2\theta = 25.95^{o}$, 31.83^{o}, 33.02^{o}, 34.11^{o}, 39.93^{o} corresponding to the (002), (211), (300), (202) and (310) diffraction planes of crystalline HA (JCPDS 9–432) while the PMMA appeared more amorphous morphology than HA. The diffraction pattern of bulk PMMA was consistent with a previous report[36], showing broad peaks at 14.2° and 29.9°, indicating the amorphous state of PMMA (Figure 5).

3.5 In vitro cell cytotoxicity

An ideal bone substitute should not release toxic products or produce adverse reactions that can be evaluated through in vitro cytotoxic tests. The level of toxicity of CS-HA/PMMA composites cultured for different periods of time towards viability of fibroblasts cells was evaluated using ISO10993-5 standard test method of indirect MTT cytotoxicity assay and the results are presented in Figure 6. As can be seen, the cell viability data showed that the addition of the as-prepared CS-HA/PMMA scaffolds into the cell culture demonstrated no significant toxicity ($p > 0.05$) to the cell viability when compared with negative control and the average absorbance values were almost equal to that of the control condition. However, slight reductions in the optical density (OD) values were observed for the RCM. This may due to the disorder of chitosan. It could be seen from Figure 6, the average viability of fibroblasts cells cultured on CS-HA/PMMA composites reached above 80% which meant fibroblasts cells might occupy all available spaces on the CS-HA/PMMA composites. The obtained results suggested that CS-HA/PMMA composites were nontoxic to L929 cells.

Figure 7 corresponded to the cell attachment and proliferation studies of L929 cells. A, B, C , D, E, F, G and H corresponded to the SEM images of cell attachment on the prepared bone scaffolds with different chitosan content and different prefrozen methods respectively. The SEM images showed that the biocompatibility and cell proliferation of the bone scaffolds were all good. The cells appeared to adhere on the surface well and exhibited a normal morphology on the surface of the CS-HA/PMMA composites. The images also showed that the number of cells increased with the increase of chitosan content in the composites. Chitosan and hydroxyapatite played a role in enhancing the activity of L929 cells. These data indicate that the composite scaffolds showed enhanced biocompatibility with the increase of chitosan content. The biocompatibility and cell proliferation of the bone scaffolds show the same trend. The number of the cell on the scaffolds prepared by different prefrozen method with the same chitosan concentration were almost the same. This also demonstrated that the prefrozen method had no significant influence on the biocompatibility of the CS-HA/PMMA composites.

4. Conclusions

In this paper, a series of CS-HA/PMMA composites with good mechanical properties were fabricated by freeze drying method and free radical polymerization. The prefrozen method had significant influence on the mechanical properties of the materials. The prepared bone scaffolds were characterized using TGA and SEM. Porosity of the CS-HA scaffolds were evaluated. It showed that prefrozen method and chitosan concentration had significant influence on the morphology and mechanical property of bone scaffolds. The porosity and compression modulus of CS-HA scaffolds prefrozen at -40 ℃ were higher than those prefrozen in liquid nitrogen. The porosity of the scaffolds decreased as the increase of chitosan content. On the contrary, as the increase of chitosan content, the compression modulus increased significantly, the cell proliferation also became better. The prefrozen method had no significant influence on the thermal behaviour.

Acknowledgement

We gratefully acknowledge the financial support from National Natural Science 382 Foundation of China (Grant No. 21304005) and Jiangsu Provincial Natural Science 383 Foundation (Grant No. BK20131145).

Notes and references

1 R. Murugan and S. Ramakrishna, *Biomaterials*, 2004, **25**, 3829;
2 W. R. Moore, S. E. Graves and G. I. Bain, *ANZ Journal of Surgery*, 2001, **71**, 354;
3 Y. Cheng, X. Luo, J. Betz, G. F. Payne, W. E. Bentley and G. W. Rubloff, *Soft Matter*, 2011, **7**, 5677;
4 J. J. Chris Arts, N. Verdonschot, B. W. Schreurs and P. Buma, *Biomaterials*, 2006, **27**, 1110;
5 J. M. Holzwarth and P. X. Ma, *Biomaterials*, 2011, **32**, 9622;
6 M. C. G. ´rrez, M. Jobbágy, M. L. Ferrer and F. d. Monte, *Chemistry of materials*, 2008, **20**, 11;
7 M. Fosca, V. S. Komlev, A. Y. Fedotov, R. Caminiti and J. V. Rau, *ACS applied materials & interfaces*, 2012, **4**, 6202;
8 L. Bi, W. Cheng, H. Fan and G. Pei, *Biomaterials*, 2010, **31**, 3201;
9 S. W. Choi, J. Xie and Y. Xia, *Advanced materials*, 2009, **21**, 2997;
10 J. Mitra, G. Tripathi, A. Sharma and B. Basu, *RSC Advances*, 2013, **3**, 11073;
11 S. W. Choi, J. Xie and Y. Xia, *Advanced materials*, 2009, **21**, 2997;
12 L. C. Palmer, C. J. Newcomb, S. R. Kalt, E. D. Spoerke and S. I. Stupp, Chemical Reviews, 2008, **108**, 4754;
13 L. L. Hench, *Journal of the American Ceramic Society*, 1998, **18**, 1705;
14 L. Chen, J. Hu, J. Ran, X. Shen and H. Tong, *RSC Advances.*, 2015, **5**, 56410;
15 F. Scalera, F. Gervaso, K. P. Sanosh, A. Sannino and A. Licciulli, *Ceramics International*, 2013, **39**, 4839;
16 Q. Wu, X. Zhang, B. Wu and W. Huang, *Ceramics International*, 2013, **39**, 2389;
17 L. Jiang, Y. Li, X. Wang, L. Zhang, J. Wen and M. Gong, *Carbohydrate Polymers*, 2008, **74**, 680;
18 J. R. Woodard, A. J. Hilldore, S. K. Lan, C. J. Park, A. W. Morgan, J. A. Eurell, S. G. Clark, M. B. Wheeler, R. D. Jamison and A. J. Wagoner Johnson, *Biomaterials*, 2007, **28**, 45;
19 M. a. C. Gutiérrez, Z. Y. Garcia-Carvajal, M. a. J. Hortiguela, L. Yuste, F. Rojo, M. a. L. Ferrer and F. del Monte, J*ournal of Materials Chemistry*, 2007, **17**, 2992;
20 L. Qian, F. H. Zhang, *Journal of Chemical Technology and Biotechnology*, 2011, **86**, 172;
21 G. Jo, W.-K. Hong, J. I. Sohn, M. Jo, J. Shin, M. E. Welland, H. Hwang, K. E. Geckeler and T. Lee, *Advanced materials*, 2009, **21**, 2156;
22 S. Deville, *Science*, 2006, **311**, 515;
23 C. Jiang, Z. Wang, X. Zhang, X. Zhu, J. Nie and G. Ma, *RSC Advances*, 2014, **4**, 41551;
24 P. Jithendra, A. M. Rajam, T. Kalaivani, A. B. Mandal and C. Rose, *ACS applied materials & interfaces*, 2013, **5**, 7291;
25 J. Han, G. Ma and J. Nie, *Materials Science and Engineering: C*, 2011, **31**, 1278;
26 Y. Zhang, J. R. Venugopal, A. El-Turki, S. Ramakrishna, B. Su and C. T. Lim, *Biomaterials*, 2008, **29**, 4314;
27 T. Almeida, B. J. M. Leite Ferreira, J. Loureiro, R. N. Correia and C. Santos, *Materials Science and Engineering: C*, 2011, **31**, 658;
28 R. Kang, Y. Luo, L. Zou, L. Xie, H. Lysdahl, X. Jiang, C. Chen, L. Bolund, M. Chen, F. Besenbacher and C. Bünger, *RSC Advances*, 2014, **4**, 5734.
29 M. S. Fernandez, J. I. Arias, M. J. Martinez, L. Saenz, A. Neira-Carrillo, M. Yazdani-Pedram and J. L. Arias, *Journal of tissue engineering and regenerative medicine*, 2012, **6**, 497-504.
30 C. Jiang, Z. Wang, X. Zhang, X. Zhu, J. Nie and G. Ma, *RSC Advanced.*, 2014, **4**, 41551;
31 J. R. Woodard, A. J. Hilldore, S. K. Lan, C. J. Park, A. W. Morgan, J. A. Eurell, S. G. Clark, M. B. Wheeler, R. D. Jamison and A. J. Wagoner Johnson, *Biomaterials*, 2007, **28**, 45;
32 J. Wu and J. C. Meredith, *ACS Macro Letters*, 2014, **3**, 185;
33 M. Matsumoto, S. Saito and I. Ohmine, *Nature*, 2002, **416**, 409;
34 K. M. Pawelec, A. Husmann, S. M. Best and R. E. Cameron, *Applied Physics Reviews*, 2014, **1**, 021301;
35 M. Akyurt, G. Zaki and B. Habeebullah, *Energy Conversion and Management*, 2002, **43**, 1773;
36 Y. Li, B. Zhang, X. Pan, *Composites Science and Technology*, 2008, **68**, 1954.

Journal Name

ARTICLE

Table 1 Sample codes and porosity of different samples

Sample code	Chitosan / g	HA /g	Acetic acid / g	Porosity (SCM)	Porosity (RCM)
CS-3/HA-10	3	10	87	62.1	51.7
CS-6/HA-10	6	10	84	55.3	47.0
CS-9/HA-10	9	10	81	50.3	45.8
CS-12/HA-10	12	10	78	47.0	33.8

Figure 1 SEM images of the interconnected structure of HA/chitosan porous scaffolds with different CS concentrations by using different prefrozen methods. (a) CS-3/HA-10 scaffolds prepared by SCM, (b) CS-6/HA-10 scaffolds prepared by SCM ,(c) CS-9/HA-10 scaffolds prepared by SCM, (d) CS-12/HA-10 scaffolds prepared by SCM, (e) CS-3/HA-10 scaffolds prepared by ECM (f) CS-6/HA-10 scaffolds prepared by RCM, (g) CS-9/HA-10 scaffolds prepared by RCM, (h) CS-12/HA-10 scaffolds prepared by RCM.

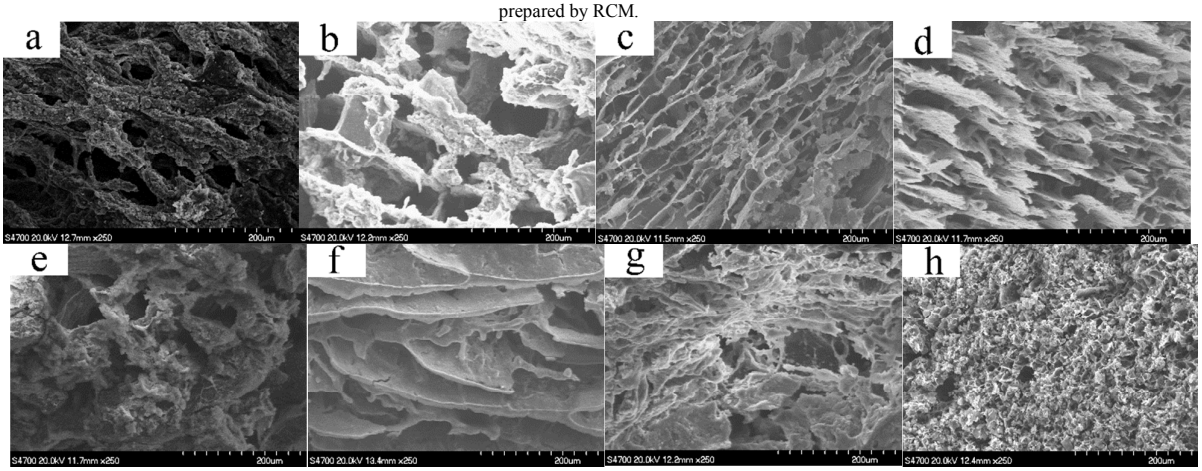

Scheme 1 The scheme of chitosan dissolution process in acetic acid

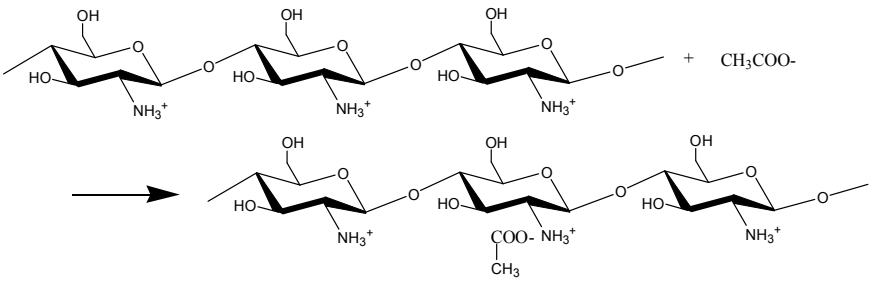

Figure 2 Mechanism for formation of chitosan network structures and mechanism for formation of chitosan network structures

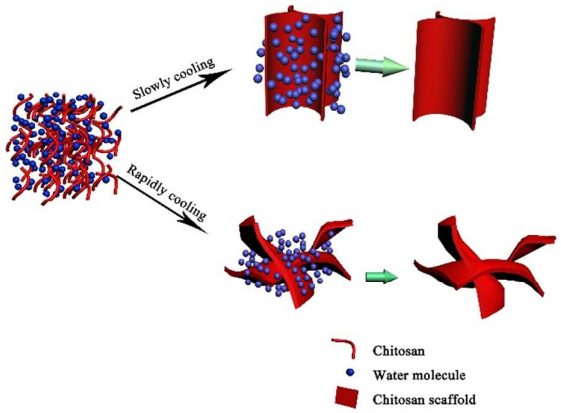

Figure 3 TGA (a) and DTG (b) curves of bulk PMMA and CS-12/HA/PMMA bone composite.

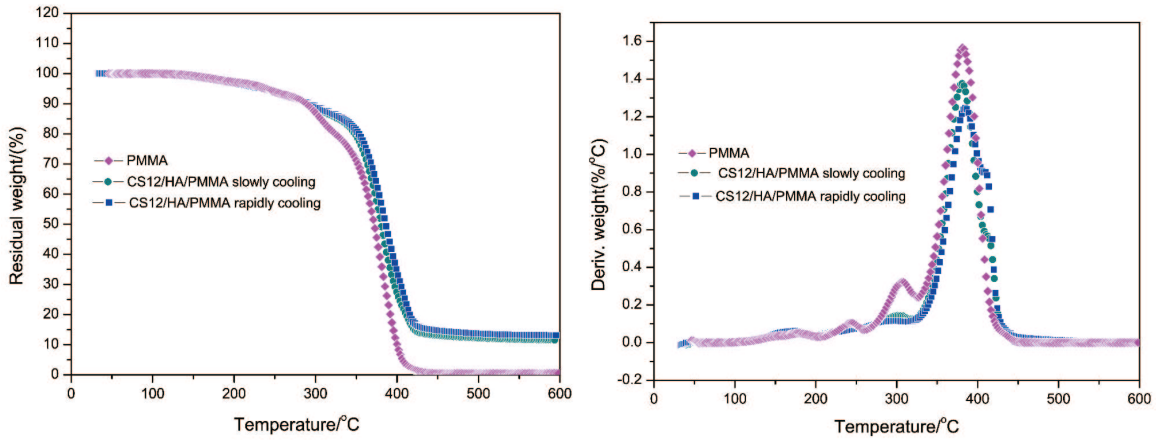

Figure 4 The compression modulus of CS-HA/PMMA composites

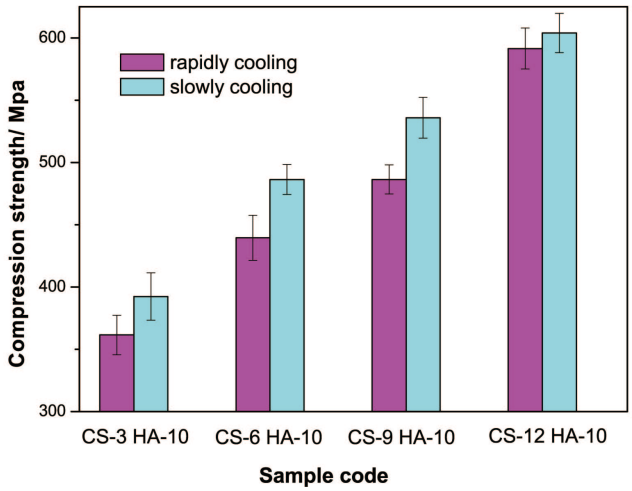

Figure 5 The XRD spectrum of bulk PMMA and CS-12-HA/PMMA bone composites prepared by SCM and RCM

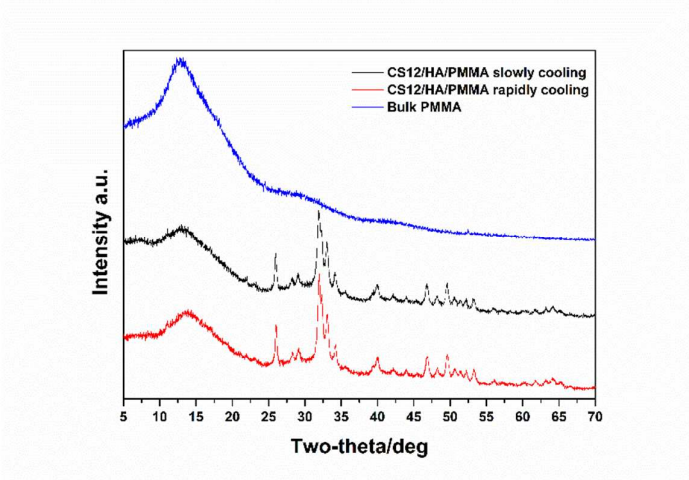

Figure 6 Cell viability study of the bone substitutes

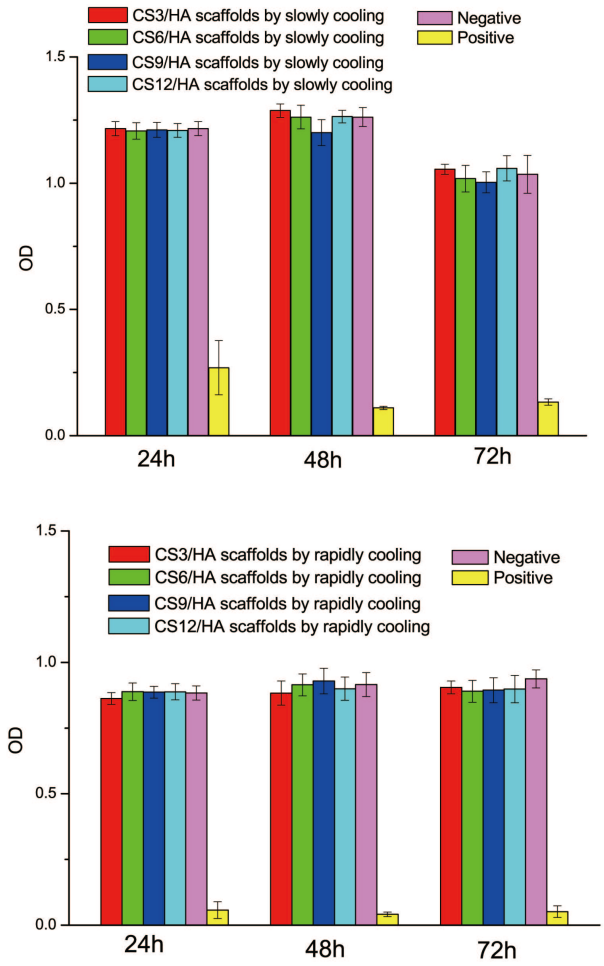

Figure 7 SEM images of cell attachment of bone substitutes (A) CS-3/HA-10 scaffolds pre-frozen by SCM, (B) CS-6/HA-10 scaffolds pre-frozen by SCM, (C) CS-9/HA-10 scaffolds pre-frozen by SCM, (D) CS-12/HA-10 scaffolds pre-frozen by SCM, (E) CS-3/HA-10 scaffolds pre-frozen by RCM, (F) CS-6/HA-10 scaffolds pre-frozen by RCM, (G) CS-9/HA-10 scaffolds pre-frozen by RCM, (H) CS-12/HA-10 scaffolds pre-frozen by RCM

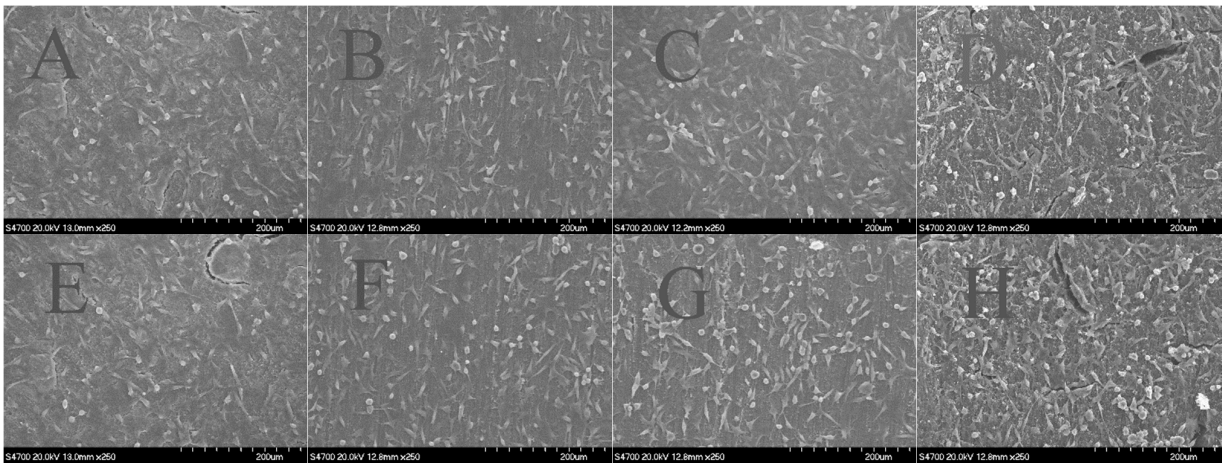

Table of contents entry

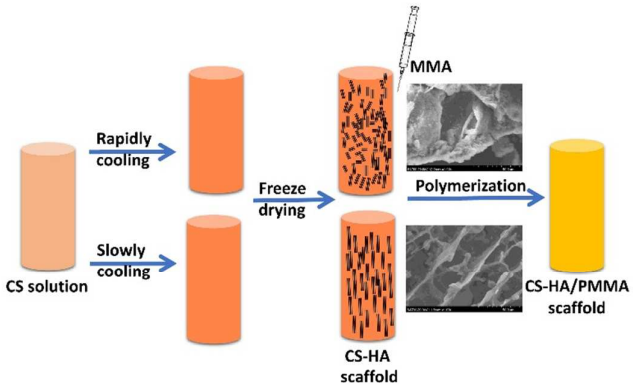

The process of different prefrozen method for preparing CS-HA/PMMA scaffold for bone tissue engineering